Journal of
Engineering Sciences
Faculty of Engineering
Assiut University
JES
مجلة
العلوم الهندسية
كلية الهندسة
جامعة أسيوط
journal homepage: http://jesaun.journals.ekb.eg

Short-Term Efficiency of Using Sustainable BFRP Bars in Post-Tensioning Systems for One-Way RC Slabs

Received 23 June 2023; Revised 29 August 2023; Accepted 1 September 2023

Sameh Yehia[1]
Sayed Abd El-Baky[2]
Abdullah Haded[3]
Arafa M. A. Ibrahim[4]

Keywords
Post-tensioning System, Basalt FRP, Hybrid Reinforcement, RC Slab Strengthening, Near Surface Mounted

Abstract
Basalt Fiber Reinforced Polymer (BFRP) bars are manufactured from sustainable natural materials. BFRP Young's modulus constitutes weak performance to the serviceability limits in the structural reinforced concrete (RC) elements, but using post-tensioning systems controls the serviceability limits. Nine RC slabs were tested under a four-point bending scheme. However, the efficiency of using the BFRP post-tensioning system bars as a main reinforcement of RC slabs was evaluated in two different stress levels of 10% and 50% of the rupture strength of the bars. Also, the near-surface mounted (NSM) external strengthening post-tensioning BFRP system by two different stress levels of 10% and 30% of the rupture strength was investigated. Additionally, the hybrid reinforcement performance of both steel and BFRP bars was studied. The relevant results showed that the post-tensioning BFRP systems significantly enhanced the ultimate load and vertical deflection of the RC slabs if the stress level was 50% and 30% for the internally reinforced and externally strengthened slabs, respectively. BFRP bars in hybrid RC slabs achieved more energy absorption. At the same reinforcement area, the internal bonded BFRP bars can achieve a higher ultimate load than the unbonded external BFRP bars by 11%. Furthermore, the increment rate in prestressing losses for RC slabs with higher prestressing levels of BFRP bars was less than that of slabs with lower prestressing levels of BFRP bars. Consequently, the efficiency of the external post-tensioning system was 95.78% for the RC slab with a 50% stress level after 1000 hrs, and it's recommended as a design guideline.

1. Introduction

The pre-stressed precast slab systems with either steel bars or fiber reinforced polymer (FRP) bars has many advantages over ordinary reinforced concrete (RC) ones. Comparing with the ordinary RC slabs, the precast pre-stressed systems have superior behavior in terms of the strength and

[1] Assoc. Professor, Dept. of Civil. Eng., Faculty of Engineering, Suez University, Egypt. s.yehia@suezuni.edu.eg
[2] Professor, Strength & Properties of Materials, Housing & Building National Research Center, Egypt. s_elbakey@yahoo.com
[3] MSc, Dept. of Civil Eng., Faculty of Engineering, South Valley University, Egypt. ab.t@hotmail.com
[4] Assist. Professor, Dept. of Civil Eng., Faculty of Engineering, South Valley University, Egypt. arafamai2015@gmail.com

https://doi.org/10.21608/JESAUN.2023.219637.1241

serviceability limit states; i.e., by adopting these systems, the slabs can cover long spans with allowable cracks' width and deflections, besides the short construction periods. Many researchers have studied the behavior of precast and post-tensioned RC systems for different material types of reinforcement. E.g., **[1]** studied how basalt FRP (BFRP) bars act when exposed to long static loading by 50% of the ultimate strength capacity of the BFRP bar (f_u). The BFRP bars plateaued much like the steel bars after an initial elongation of 0.5 mm, and they even retained their load better than steel bars for all of the loading stages that were recorded. The results revealed that the prestress losses in BFRP and steel bars are equal or less than those in steel cable. However, the creep behavior of the BFRP bar is different from that of steel since the creep results for BFRP and steel are similar for the time and stages of loading. On the other hand, BFRP materials have an excellent strength-to-weight ratio and lower environmental impact, and these behaviors were investigated by **[2]**. They tested BFRP bars with a diameter of 4.3 mm to loads that ranged from $0.2f_u$ to $0.8f_u$ in order to study the creep rupture. In order to simulate exposure of the FRP bars to the alkaline environment of concrete, an alkaline solution with a pH of around 13 was utilized. This simulation was carried out at a high temperature of 60°C to hasten the degradation process. Based on their study, the ultimate creep rupture strength coefficients of the BFRP bars were calculated to be approximately 18% for a 50-year service life and 28% for a 5-year service life. According to estimates, the appropriate million-hour creep coefficient is 13%. Those estimated creep rupture strength coefficients are based on the properties of the studied BFRP bars and may vary. The authors **[3]** carried out some long-term investigation on six BFRP pre-tensioned concrete beams to three prestress levels of 20%, 30%, and 40% of the ultimate tensile load capacity of the bars. According to the results of continuous strain monitoring, there was an average reduction of 7% of the initial strain during the first 90 days of unloaded monitoring. An additional 0.3% reduction was observed during the period of the following six months of monitoring under continuous loading.

In general, basalt is sustainable and forms more than 90% of all igneous rocks and this is confirmed by **[4]** who stated that the embodied emissions of BFRP beams are half of that of steel-reinforced beams. In another study, the researchers **[5]** stated that the BFRP bar with highly creep rupture stress of $0.6f_u$, is a superior material for prestressing applications. The authors proposed a method to control the creep strain and reduce prestressing loss. The experimental parameters, such as pretension stress levels and duration were investigated to explore their impacts on creep strain control. The study extended to include modeling of long-term creep behavior using a semi-logarithmic equation. According to the studied specimens, pretension can substantially decrease the creep strain on BFRP tendons. Pretension stress of $0.6f_u$ for 3 hrs. duration achieves the significant creep strain control effect. The results of the residual strength in the tested specimens after the creep test were consistent with the aforementioned control effects. According to the predicted modeling, with a sustained stress of $0.5f_u$, the creep strain rates at 1000 and 1,000,000 hrs. for the BFRP tendon may be controlled to 1.46% and 3.65%, respectively. Furthermore, this method of enhancement (pretension process) was verified and confirmed by **[6]**. They explored the behavior of tendons reinforced with basalt fibers and subjected to three levels of initial stresses: $0.4f_u$, $0.5f_u$, and $0.6f_u$. Each relaxation test group included three specimens that were tested and lasted a total of 1000 hrs. The proposed test setup prevented slippage at the anchor zone's potential influence on the relaxation value. According to the test results, relaxation increases as prestressing load increases, but for the first 10 hrs., there were not any noticeable differences between the relaxation values for the various initial stresses. The relaxation rates for the initial stress level of $0.6f_u$ are much higher than those for $0.4f_u$ and $0.5f_u$ during the period from 10 hrs. to 480 hrs. for the levels of stress $0.4f_u$, $0.5f_u$, and $0.6f_u$, respectively, the relaxation rates obtained in the experiments were 4.2%, 5.3%, and 6.4% at 1000 hrs.

The authors **[7]** stated that the BFRP tendon's 50-year relaxation rate would be 11% after conducting relaxation tests on BFRP tendons with durations of more than 2000 hrs. at an initial load of $0.5f_u$. Considering that the adopted BFRP tensile strength was only 1000MPa, the possible failure of slippage at anchorage and the low volume fraction of BFRP contributed to the unusually high relaxation. The researchers **[8]** investigated the size of the overall loss rate, the law of prestressing short-term loss, and the distribution of prestressed loss over time in the total prestressed loss of carbon fiber reinforced polymer (CFRP) bars. The results of the study indicated that for older bridges with a service life of more than ten years, the total prestress loss rate of external prestressing reinforcement of CFRP bars is between 4% to 8%, with the majority of the loss occurring within seven days of the prestressing. Additionally, the anchorage loss of CFRP bars is the primary cause of the short-term prestressing loss in the external prestressing of prestressed CFRP bars for the strengthening of older bridges. The anchorage loss accounts for approximately 45.90% of the elastic compression loss of concrete, which is extremely minimal and may virtually be ignored.

A few natural frequencies to illustrate the numerical results of prestress loss in prestressed hollow core slabs was presented by **[9]**. A 3D finite element approach has been used to analyze prestress loss. According to the results of the study, the maximum initial stress that can be placed on a strand to achieve the required frequency percentage change of 5% has been established. The authors **[10]** studied experimentally and numerically the flexural behavior of strengthened cracked or uncracked RC beams using an external post-tensioning technique with stress levels of $0.1f_u$, $0.2f_u$, and $0.3f_u$ using the glass fiber reinforced polymer (GFRP) bars under the effect of cyclic loads. Further, the authors presented and utilized an innovative anchorage system for fixing the post-tensioning system. The relevant results achieved significant enhancement in the studied beams and the success of using this anchorage system in retaining the stress level of the post-tensioning force inside the tensioned GFRP bars.

The flexural behavior of reinforced concrete one-way slabs strengthened with external post-tensioning FRP tendons was studied by **[11]**, and the results revealed that this method improves the first-cracking moment, the moment at bar yielding, and the ultimate moment, as well as the stiffness of the slab throughout the loading process. Due to external tendon strengthening, the slabs used in this study had maximum first-cracking and ultimate moments increments of 121% and 103%, respectively compared with unstrengthened slabs. External tendons improve the ultimate strain in the top concrete fiber by reducing the tensile stresses in the concrete and the bonded reinforcement, making the cracks narrower and denser. The benefits of the suggested technology are also enhanced by increasing the prestressing force and the number of external tendons. The researchers **[12]** stated that the most part of relaxation loss occurred within the first hours of applying prestressing in bars. Also, the authors **[13]** declared that the results obtained showed a direct relationship between the pre-tensioning limit and the FRP composites' ability to relax. However, regardless of the initially applied stress, aramid fibers often relax. The uniaxial tensile tests on the carbon and aramid samples revealed that the loss of prestressing force between 3.5 and 17 years was essentially nonexistent. The first 100 hrs. exhibited the highest fall in load, while subsequent drops were minimal. GFRP composites have excellent relaxation characteristics at low-stress levels, although it's creep-sensitivity.

The creep behavior of BFRP tendons for prestressing application was investigated by **[14]**. The experimental program was relevant to the relationship between creep strain and time, creep rate, and residual strength. Furthermore, statistical analysis was used to predict the creep rupture stress. The results showed that under modest levels of stress, the BFRP tendons' creep rate remains steady with low values. Whilst, the BFRP's residual strength is still close to 95% of its initial tensile strength after 1000 hrs. of sustained load, and the corresponding coefficient of variation is

significantly lower than the initial coefficient of variation. Furthermore, the creep rupture stress limit for BFRP tendons for prestressing applications can be adopted up to 52% of its tensile strength. The authors also noted that the first stage of the rapid creep strain development of the BFRP tendon completely ended within the first 72 hrs. under a sustained stress of $0.5f_u$ to $0.65f_u$, then developed much slower. The average proportion of the creep strain was approximately 74% at the duration of 72 hrs. in the total creep strain at 1000 hrs.

As a summary of the aforementioned review of the existing studies, it may be concluded that: BFRP has good physical and mechanical properties that make it an attractive material for internal or external reinforcement of the RC elements with acceptable serviceability limits that may be further improved using the post-tensioning system; the post-tensioning external unboned system would be a possible method for limiting the deflections and cracking of BFRP-reinforced flexural RC elements, and this system is capable of restressing, distressing, and exchanging any external prestressing at any maintenance stage. Despite the advantages of BFRP compared with other composites, it is clear that there is a lack of experimental and analytical investigations of post-tensioned BFRP slabs. Moreover, to the authors' best knowledge, the national and international codes of practice do not have provisions for the design of slabs reinforced with BFRP bars and slabs with post-tensioning BFRP systems. As a result, research efforts towards developing design guides for such kinds of RC slabs are essential. The present research is a contribution in this direction. Consequently, the main objectives of this study were to: investigate the behavior of RC slabs internally reinforced with hybrid steel and BFRP bars; investigate the efficiency of BFRP post-tensioning systems in RC slabs as main reinforcement or external strengthening using the near-surface mounted (NSM) technique; compare the structural responses of the slabs with different reinforcement and giving design guidelines for the best behavior. In order to achieve the objectives, an extensive experimental program is firstly carried out on RC slabs and analytical calculations of the stress losses in the post-tensioning BFRP bars according to different codes **[15-19]** is finally adopted to verify the efficiency of using this system.

2. Validity of Used Materials

Natural crushed stone was used as coarse aggregate from the attaka quarry in Egypt, and natural sand from the pyramid quarry in Egypt was used as a fine aggregate. The used coarse and fine aggregate were tested according to **[20]**, and the obtained test values are within the acceptable limitations, as shown in **Tables 1 and 2**. Portland cement CEMI 42.5-N was used to produce the concrete mix and was tested according to **[21]**. The appendages, physical and mechanical properties of the used cement are shown in **Table 3**. Also, drinking water was used for concrete mixing and curing of the RC slabs. On the other hand, the ingredients of the concrete mix were designed according to **[22]** for producing compressive strength of concrete of 35 MPa and the proportions of the concrete ingredients expressed as summarized in **Table 4**. Further, trial mixes were cast to evident the selected compressive strength value after twenty-eight days.

The properties of FRP reinforcements vary with fiber volume fraction ratio and the bar diameter. Contrary to steel reinforcement, the tensile strength of FRP bars is a function of the bar diameter due to shear lag, which causes outer diameter fibers to experience more stress than fibers on the inside of the cross-section of the FRP bar. Consequently, as the diameter of the bar increase, the tensile normal stress varies across the cross-section due to shear lag developing between the yarns of fibers, see **Fig. 1**. Ultimately, larger diameter bars could experience reduced strength and inefficiency, as stated in the study **[23]**. Hence, in the current research, BFRP bars were chosen to be 10 mm in diameter with high volume fraction to reduce the stress losses.

The BFRP bars were manufactured by pultrusion of sustainable natural basalt continuous and thermosetting unsaturated polyester resin with peroxide as a catalyzer. The tensile strength test for

five samples of BFRP bars with total length of 800 mm was done by embedding the BFRP bar into steel hollow tubes (300 mm length) filled with epoxy material **[24]** for the gluing length of 200 mm. The prepared bars were kept for ten days (according to the datasheet of the used epoxy) before testing to confirm the epoxy cure. The mechanical properties obtained from the tensile strength test according to **[25-27]**. The volume fraction of BFRP bar was calculated according to **[27]**. Tensile strength, tensile modulus, elongation percentage, and volume fraction are presented in **Table 5**. Furthermore, the used longitudinal steel reinforcement was 10 mm in diameter and was tested according to **[28]**. Both proof and ultimate strengths for the selected diameter are listed in **Table 6**.

Table 1: Physical and mechanical properties of the used crushed stone

Property	Result	Acceptable Limit [20]
Specific Gravity	2.65	-
Unit Weight (t/m^3)	1.68	-
Materials Passing No. 200 Sieve (%)	1.35	Less than 3%
Absorption (%)	1.44	Less than 2.5%
Abrasion (Los Anglos) (%)	14.82	Less than 30%
Crushing Factor (%)	16.71	Less than 30%
Impact (%)	17.87	Less than 45%
Maximum Aggregate Size (mm)	20	-
Fineness Modulus	6.68	-

Table 2: Physical properties of the used sand

Property	Result	Acceptable Limit [20]
Specific Gravity	2.58	-
Unit Weight (t/m^3)	1.56	-
Materials Finer than No. 200 Sieve (%)	1.85	Less than 3%
Absorption (%)	1.25	Less than 2%
Zone	1	-
Fineness Modulus	2.53	-

Table 3: Physical and mechanical properties of cement

Property		Result	Specification Limits [21]
Soundness (mm)		4	Not more than 10mm
Fineness of Cement (cm^2/gram)		3190	-
Specific Gravity		3.15	-
Setting Time (minutes)	**Initial**	170	Not less than 60Minutes
	Final	220	-
Compressive Strength (MPa)	**2 days**	22.7	Not less than 10MPa
	28 days	56.4	Not less than 42.5MPa and not more than 62.5MPa

Table 4: Proportion of concrete ingredients [22]

(f_{cu}) (MPa)	Cement (kg/m^3)	Fine Aggregate (kg/m^3)	Coarse Aggregate (kg/m^3)	Water ($Liter/m^3$)
35	450	608.7	1126	202

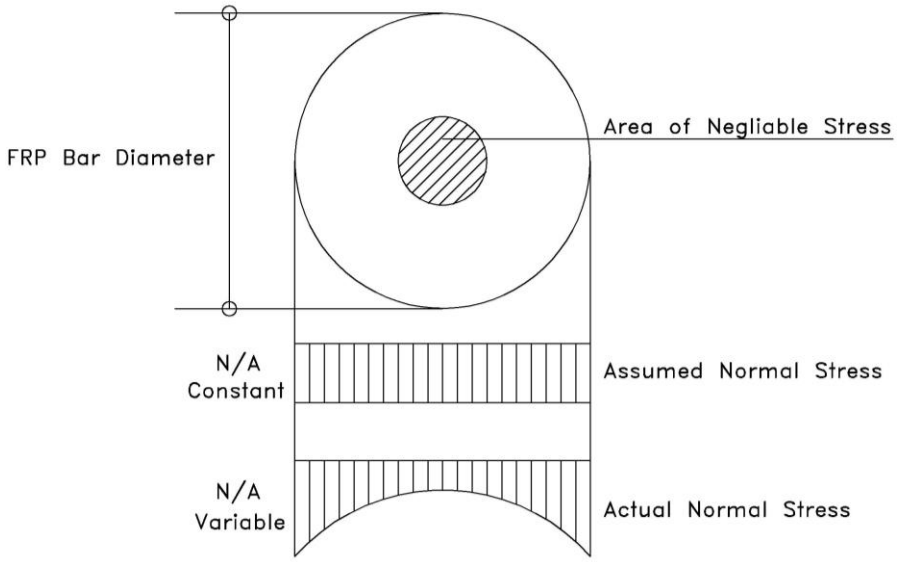

Fig. 1: Normal stress distribution across cross-sectional area of FRP reinforcement bar

Table 5: Mechanical properties of BFRP bars [25-27]

Type	Diameter (mm)		Tensile Strength (MPa)	Modulus of Elasticity Bar (GPa)	Elongation (%)	Volume Fraction V_F (%)	Modulus of Elasticity (GPa) Resin
	Nominal Diameter	Actual Diameter by Digital Caliper					
BFRP Bars	10	9.5	835	55.7	1.5	71	3.5*

* Datasheet of BFRP bars.

Table 6: Mechanical properties of the used steel reinforcement bar

Properties	Measured Values	Minimum Specification Limit [28]	Minimum Specification Limit [29]
	High Grade Steel B420C-R	High Grade Steel B420C-R	Grade 60
Yield/Proof Stress	481MPa	420MPa	420MPa
R_m/R_{eH}	1.26	1.15	-
% of Elongation	20.45%	14%	9%

3. Experimental Program

3.1. Details of the Tested Specimens

Nine RC slabs with a rectangular cross-section of 500 mm width, 120 mm thickness, and an overall span of 3000 mm were tested under the effect of a four-points bending moment. The slabs are classified into four categories. The first category consisted of two RC slabs representing the control reinforced with only one type of reinforcement: namely (S-St-Control) and BFRP bars (S-BF-Control). The second category was carried out to study the effect of using a post-tensioning system

for embedded BFRP bars as a main reinforcement with different levels of stress 10% and 50% (S-BF-10%-Int. and S-BF-50%-Int., respectively). The third one aimed to clarify the performance of strengthened RC slabs by NSM techniques under the effect of external post-tensioning systems with different values of stress levels: 0%, 10%, and 30% (S-St-BF-zero%-Ext., S-St-BF-10%-Ext. and S-St-BF-30%-Ext., respectively). And finally, the fourth one was performed to study the effect of using hybrid reinforcement for RC slabs (S-St-BF, and S-St-St). **Table 7**, shows the details of the RC slabs. It is worth mentioning that, the maximum level of prestressing up to 50% of the ultimate strength of BFRP was selected based on the recommendations of **[17]** which stated in the overall design approach section. The applied stress levels in the post-tensioning bars were checked for compression failure at the bottom fiber of the RC slab and found to be less than the compression failure stress of concrete. Also, the cracking tensile stress was calculated according to **[15]** and compared to the tensile bending stress at the top fiber of the RC slab to check the appearance of the first crack. It is found that the applied tensile bending stress due to the applied stress levels in the post-tensioning bars is less than the cracking tensile stress. On the other hand, effective depth plays a major role in determining the ultimate load of the tested RC slab. Further, the effective depth for the internal reinforcement was 98 mm to facilitate the installation of the external post-tensioning system to achieve the NSM technique, except for the control RC slab with traditional steel reinforcement was 105 mm. That is to verify the possibility of BFRP bars overcoming the smaller effective depth and exceeding the ultimate load of the traditional RC slab.

Table 7: Details of tested RC slabs

Slab Code	Cat.	$d_{eff.)St}$ (mm)	$d_{eff.)BF}$ (mm)	As (mm^2)	A_f (mm^2)	μ (%)	A_f/A_t (%)	Post-Tensioning Technique & Stress Level
S-St-Control	Cat. (1)	105	-	3Φ10	-	0.39	-	-
S-BF-Control		-	98	-	3Φ10	0.39	-	-
S-BF-10%-Int.	Cat. (2)	-	98	-	3Φ10	0.39	-	Internal – 10%
S-BF-50%-Int.		-	98	-	3Φ10	0.39	-	Internal – 50%
S-St-BF-zero%-Ext.	Cat. (3)	98	109	3Φ10	2Φ10	0.65	0.40	-
S-St-BF-10%-Ext.		98	109	3Φ10	2Φ10	0.65	0.40	External – 10%
S-St-BF-30%-Ext.		98	109	3Φ10	2Φ10	0.65	0.40	External – 30%
S-St-BF	Cat. (4)	98	109	3Φ10	2Φ10	0.65	0.40	-
S-St-St		98	109	5Φ10	-	0.65	-	-

3.2. Manufacturing of RC Slabs

(Φ10/250 mm) was used as a secondary steel reinforcement mesh to join the main longitudinal steel reinforcement mesh. The concrete mix was produced using a mixer in the laboratory, and an electric vibrator was used to compact the concrete mix mechanically into the wooden forms. Six control standard samples, such as cubes were cast in every batch to ensure the target compressive strength for RC slabs after twenty-eight days. The RC slabs were watery cured for seven days from casting day, but standard samples were immersed in the water tank after one day from casting till the day of the testing (seven days and twenty-eight days). Standard samples were tested according to **[30]**.

3.3. Details of the BFRP Post-Tensioning, and Anchorage System

The utilized anchorage system consists of two parts. The first part is the BFRP bar, and the second part is the steel grip (plain-threaded part). The steel grip is a tube of 300 mm in length, 200 mm (plain-hollow inside), and the left length is 100 mm threaded for the washer and two nuts fixations. The BFRP bar was inserted inside the hollow tube of the steel grip and then glued with epoxy **[24]** up to 200mm embedded length to ensure a high bond between the BFRP bar and the inside surface of the hollow side in the grip (as the same idea of testing BFRP bars under tensile force **[31]**). Two or three angles 100x100x13 in mm (St.37) per side based on internal or external post-tensioning system were designed and utilized to prevent the local bearing failure in the concrete surface. Those angles help to fix the washer and two nuts with the threaded part of the anchorage system. See the following **Fig. 2**, which shows the details of the used anchorage system. The used anchorage system was also examined and achieved significant results under cyclical loading by **[10]**. It worth to be mentioning that the anchorage system was tested to develop at least 90% of the specified tensile strength according to **[19]** requirements without failure. In the end, **Fig. 3**. Shows the installation of post-tensioning systems for RC slabs.

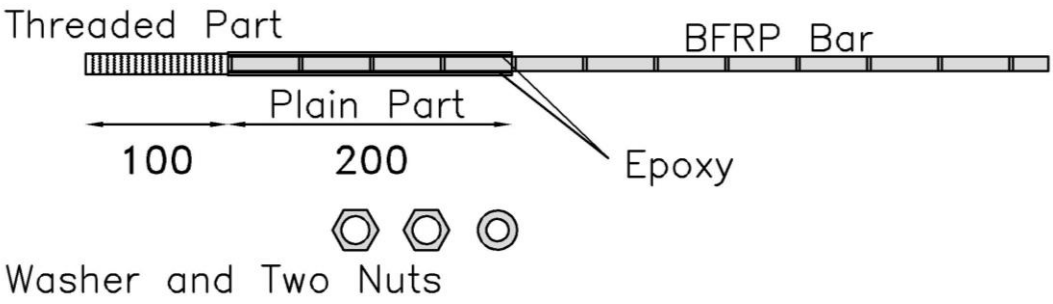

Fig. 2: Anchorage system

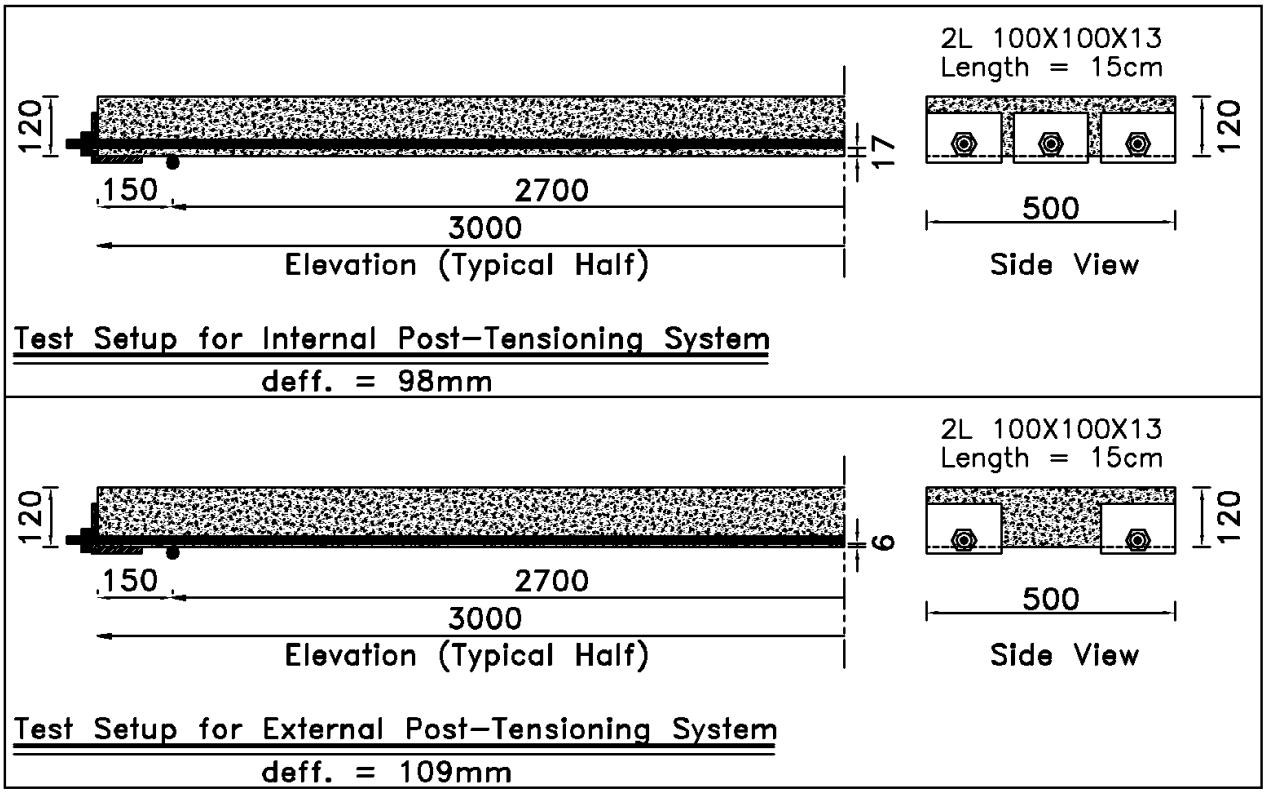

Fig. 3: Details of internal and external (NSM) post-tensioning system

3.4. Preparation and Testing of RC Slabs

After 100 hrs. from the concrete cast, the post-tensioning systems were installed with a certain level of stress according to the RC slab code. On the other hand, the RC slabs were prepared for testing after twenty-eight days (672 hrs. from the concrete cast, and 572 hrs. from installing the post-tensioning system), and the dial gauges were fixed on the bottom mid-span side of the tested RC slab to measure the vertical deflection. Two-line loads were applied to the tested RC slabs with an increment of about 5 kN using a rigid steel rod till failure. **Fig. 4** shows the typical test setup for RC slabs.

After the curing of epoxy (ten days according to the product datasheet), the washer and two nuts were installed, and the stress was applied to post-tensioning bars by one-shot using torque keys immediately at the same moment after 100 hrs. from the concrete cast to ignore the elastic shortening losses. In order to ensure the applied stress levels, the strain gauges' which were connected with strain meters monitored precisely. The used strain gauges had a 350-ohm resistance, 2.04 gauge' factor, and a length of 15mm. Whilst, the monitored strain gauge was glued on the bar surface, and the recorded strain was $1.50x10^{-3}$, $4.50x10^{-3}$, and $7.50x10^{-3}$ in the bar to generate the required stress levels 10%, 30%, and 50% of the ultimate strength capacity of BFRP bar, respectively.

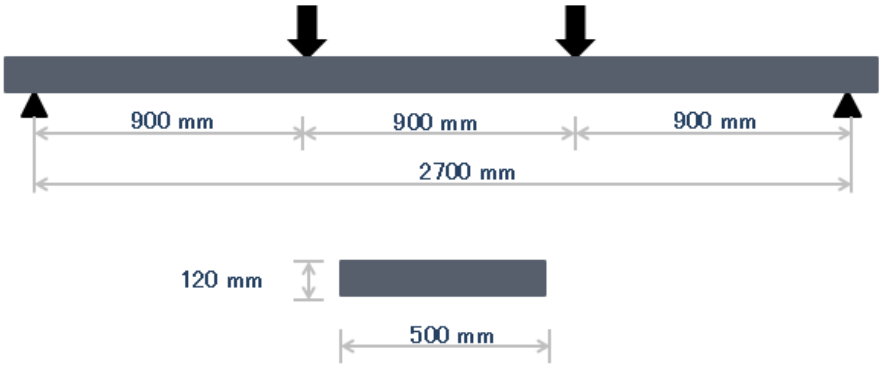

Fig. 4: Typical test setup for studied RC slabs

4. Test Results, Analysis, and Discussion

4.1. General Overview

The RC slabs were loaded until the constant load value appeared (curve plateau). That happened clearly for RC slabs with steel reinforcement. Further, the load was recorded at all stages of testing, the crack propagation was observed, and the crack pattern was classified. Table 8 shows the test results for the tested RC slabs and Table 9 shows the stiffness, and deformability indices for the tested slabs.

From **Tables 8 and 9**, it seems that the ultimate load for the RC slab S-St-Control more than the RC slabs S-BF-Control, and S-BF-10%-Int. by 119.19%, and 47.11%, respectively due to increasing of effective depth from 98 mm to 105 mm. Also, recorded more absorbed energy and ductility in comparison to the RC slabs S-BF-Control, and S-BF-10%-Int. In the pre-cracking stage, the RC slab S-BF-Control gave more stiffness than the RC slab S-St-Control due to the presences of the BFRP bars which resisting the applied loads from the beginning. It is noted that by increasing the stress level from 10% to 50% in the internal post-tensioning bars, the energy increased by 97.79% but the ductility decreased by 84.73% while the ultimate load increased by 59.40%. BFRP bars achieved desirable performance by increasing the stress level in the bars and enhanced the ultimate load of the RC S-BF-50%-Int. more than the RC S-St-Control by 8.35% and absorbed more energy by 79.81%. Although, the effective depth decreased in the last comparison by 6.67% but the RC

slab S-BF-50%-Int. overcame the lower value of the effective depth. Also, by increasing the stress levels from 10% to 50% for internal post-tensioning in the BFRP bars, the ultimate load increased by 49.00% and 137.50% in comparison to the RC slab S-BF-Control. Furthermore, the vertical deflection of the RC slabs with BFRP bars recorded highest values at the same load due to the weakness of young's modulus of the BFRP compared with steel reinforcement bars. The absorbed energy and ductility behavior significantly appeared in the RC slabs with hybrid reinforcement (steel and bonded BFRP bars) in comparison to the other RC slabs.

Table 8: Test results for the RC slabs

Slab Code	P_{cr} (kN)	P_y (kN)	P_u (kN)	P_{cr}/P_u (%)	Δ_{cr} (mm)	Δ_y (mm)	Δ_u (mm)
S-St-Control	6.02	35.07	35.07	17.20	5.71	48.12	58.02
S-BF-Control	3.00	-	16.00	18.75	0.90	-	85.00
S-BF-10%-Int.	7.06	-	23.84	29.61	7.53	-	81.05
S-BF-50%-Int.	15.00	-	38.00	39.47	10.15	-	87.00
S-St-BF-zero%-Ext.	11.00	24.00	34.00	36.67	4.00	29.50	52.00
S-St-BF-10%-Ext.	8.09	33.05	37.50	21.57	5.56	36.18	57.07
S-St-BF-30%-Ext.	10.02	40.06	48.09	20.83	3.00	25.00	44.00
S-St-BF	11.08	26.03	38.00	31.43	8.00	29.00	87.00
S-St-St	12.00	39.04	40.08	30.00	9.30	39.00	40.00

Table 9: Stiffness and deformability indices for the RC slabs

Slab Code	Stiffness (kN/mm)				Deformability	
	Initial Stiffness P_y / Δ_y	Pre-Cracking Stiffness P_{cr} / Δ_{cr}	Post-Cracking Stiffness $(P_y - P_{cr}) / (\Delta_y - \Delta_{cr})$	Post-Yielding Stiffness $(P_u - P_y) / (\Delta_u - \Delta_y)$	Energy (kN.mm)	Ductility Δ_u / Δ_y
S-St-Control	0.73	1.05	0.68	0.00	1382.77	1.21
S-BF-Control	-	3.33	-	-	781.55	-
S-BF-10%-Int.	-	0.94	-	-	1065.29	-
S-BF-50%-Int.	-	1.48	-	-	2107.04	-
S-St-BF-zero%-Ext.	0.81	2.75	0.51	0.44	1113.86	1.76
S-St-BF-10%-Ext.	0.91	1.46	0.82	0.21	1331.82	1.58
S-St-BF-30%-Ext.	1.60	3.34	1.37	0.42	1564.52	1.76
S-St-BF	0.90	1.39	0.71	0.21	2338.39	3.00
S-St-St	1.00	1.29	0.91	1.04	1263.57	1.03

It's noted from **Tables 8 and 9** that the RC slabs S-St-BF-zero%-Ext. gave ultimate load almost equal to the RC slab S-St-Control, due to the occurrence of crushing in the concrete and unbonded zero% stress level in the external BFRP bars, which force BFRP bars to work at the low load level of (24kN) after yielding of the steel reinforcement (appeared clearly in the initial stiffness and almost equal in value) and miss the benefit of using the hybrid reinforcement. On the contrary, the benefits of using BFRP bars as NSM were cleared in external post-tensioned RC slabs, by increasing the level of stress in BFRP bars from 10% to 30%, the ultimate load increased by 28.24% and vertical deflection decreased by 23.00% due to increasing of stress level in BFRP bars and higher value of the effective depth (109mm). Therefore, by increasing the stress level of the external post-tensioning BFRP bars from 10% to 30%, the ultimate load increased by 10.29%, 41.44%, respectively with an obvious reduction in the vertical deflection in comparison to the RC slab S-St-BF-zero%-Ext. The obtained results confirm the achievement of this post-tensioning system for hybrid reinforcement in NSM. The absorbed energy increased by increasing the external post-tensioning stress level from 0% to 30% by 40.46%.

Table 8 and 9, shows that the RC slab S-St-BF almost gave the same ultimate load and (P_{cr}/P_u) ratio as the RC slab S-St-St but with higher vertical deflection at the same load. Almost, all stiffness stages were equal except in the post-yielding stage the RC slab S-St-St achieved more stiffness due to the higher young's modulus for steel reinforcement. The absorbed energy for RC slab S-St-BF was more than the RC slab S-St-St by 85.06% due to the lower young's modulus of the BFRP bars. The ductility for the RC slab S-St-BF is less than the RC slab S-St-St by 16.25% due to the partial replacement of the steel reinforcement area by 40% of BFRP. Moreover, the RC slab S-St-BF-zero%-Ext. has an ultimate load less than the RC slab with hybrid reinforcement by 10.53%, both of them have the same reinforcement area (μ=0.65%) but the hybrid one has bonded BFRP bars internally. The recorded enhancement in ultimate load clarifies the effect of bonding on structural behavior.

Fig. 5, shows the relationship between the applied load and the vertical deflection. It seems that for the S-St-Control RC slab, the curve is initially linear until the appearance of the first crack at the load of 6.02kN, then the curve tilts less than the first stage by increasing the applied load, the steel bars reach to yield load at the load of 35.07kN. Ultimately, the RC slab reaches complete collapse at the load of 35.07kN. For RC slabs with BFRP bars, there is no yield that can be observed as FRP have no plastic range. The curve started by linear trend until the first crack at the load of 3.00kN, 7.06kN, and 15.00kN for S-BF-Control, S-BF-10%-Int. and S-BF-50%-Int. RC slabs, respectively. The curve tilts less than the first slope and continues with the same rate until reaches to ultimate load at 16.00kN, 23.84kN, and 38.00kN. The energy of the S-St-Control RC slab is more than BFRP RC slabs S-BF-Control and S-BF-10%-Int. due to the higher young's modulus of steel bars but the energy of the RC slab S-BF-50%-Int. more than S-St-Control RC slab. This result confirms that obtaining a significant improvement in the structural behavior can be obtained in the case of RC slab post-tensioned by 50% level of stress.

It appears from **Fig. 6** that, the relationship between the applied load and the vertical deflection for NSM external post-tensioned RC slabs. It seems that the curve has a linear trend with little degradation in slope after the first crack appears, the first crack at the load of 11.00kN, 8.09kN, and 10.02kN for S-St-BF-zero%-Ext., S-St-BF-10%-Ext. and S-St-BF-30%-Ext. RC slabs, respectively. The RC slabs remain with the extended trend of the curve until the yielding level of steel bars at the load of 24.00kN, 33.05kN, and 40.06kN and the ultimate loads were observed at 34.00kN, 37.50kN, and 48.09kN for S-St-BF-zero%-Ext., S-St-BF-10%-Ext. and S-St-BF-30%-Ext. RC slabs, respectively. BFRP bars worked significantly after the steel bars reached to the yield level, which appears significant by comparing the yield load with the ultimate load. The stiffness of the RC slabs S-St-BF-zero%-Ext., S-St-BF-10%-Ext. and S-St-BF-30%-Ext. almost in the same range

but the RC slab S-St-Control less and out of the ranged values. However, the RC slab S-St-BF-30%-Ext. have a larger energy that other RC slabs. The stiffness in all stages such as initial stiffness, pre-cracking stiffness, post-cracking stiffness, and post-yielding stiffness increased by increasing stress level in the external post-tensioning BFRP bars from 10% to 30%.

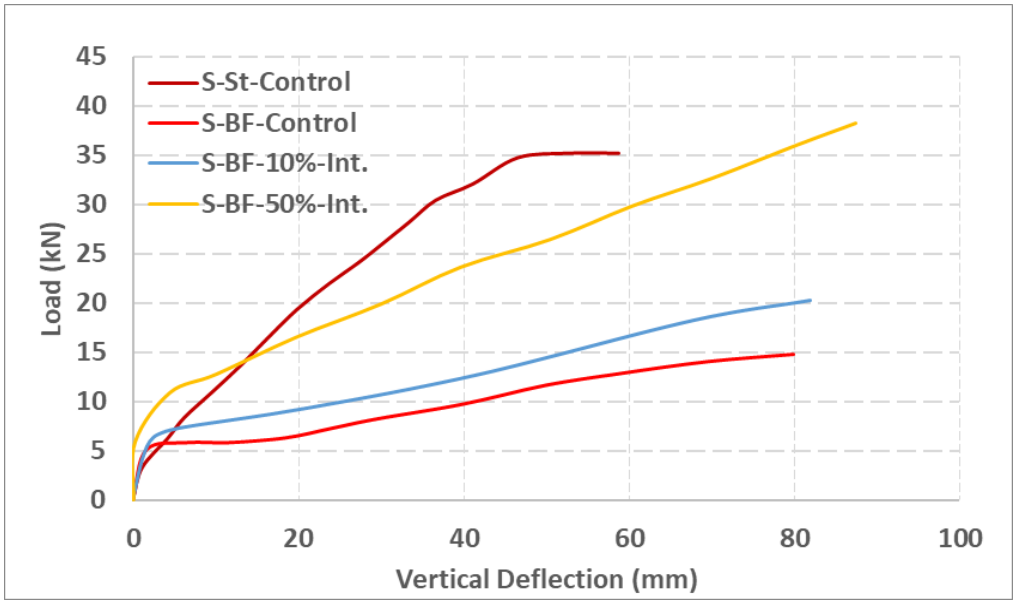

Fig. 5: Relationship between load and vertical deflection for RC slabs S-St-Control, S-BF-Control, S-BF-10%-Int. and S-BF-50%-Int.

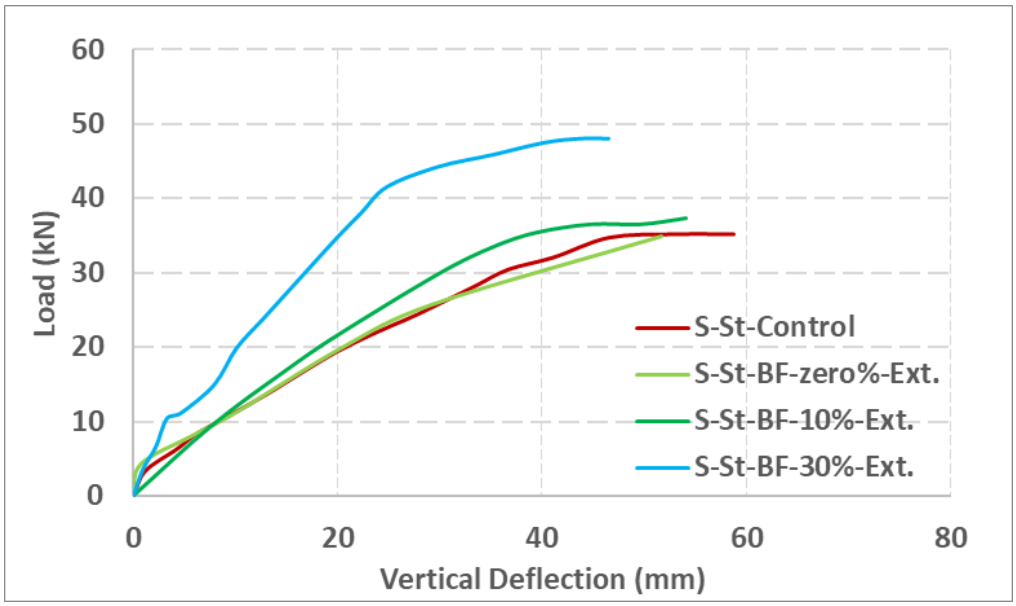

Fig. 6: Relationship between load and vertical deflection for RC slabs S-St-Control, S-St-BF-zero%-Ext., S-St-BF-10%-Ext. and S-St-BF-3%-Ext.

From **Fig. 7**, the drawn relationship behavior of the RC slabs at the beginning is similar to each other and that confirmed by initial stiffness. The first crack appeared at the load of 11.08kN and 12.00kN for S-St-BF and S-St-St. RC slabs, respectively. The yield load and the ultimate load were observed at 26.03kN and 38.04kN for the S-St-BF RC slab and 39.04kN and 40.08kN for the S-St-St RC slab. The BFRP bars did a significant improvement before yielding of steel bars and that significantly confirmed by pre-cracking stiffness. The ultimate load of the S-St-BF RC slab reached

to 38.00kN. The absorbed energy of the S-St-BF RC slab is more than S-St-St RC slab by 85.06% and that fulfills the benefits of using hybrid reinforcement with BFRP bars and adding BFRP bars as 40% of the total reinforcement area achieved the promising enhancement.

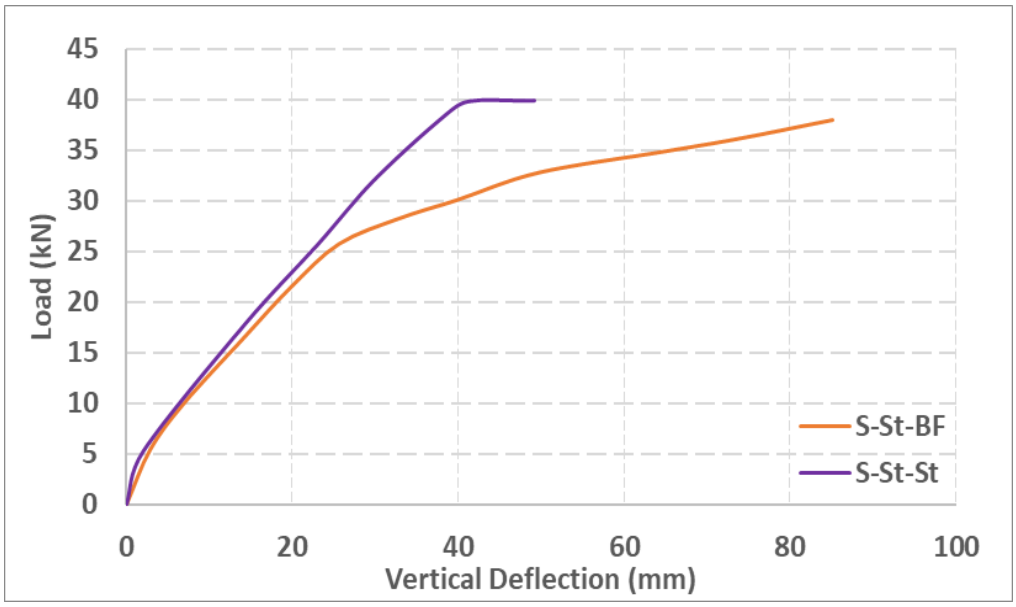

Fig. 7: Relationship between load and vertical deflection for RC slabs S-St-BF and S-St-St.

4.2. Cracks Patterns and Failure Modes

It seems from **Figs. 8 and 9** that the RC slab S-St-Control and S-BF-Control have the same crack distribution. The cracks started and spread on both sides with the same similarity. Faster development of the vertical deflection appeared in S-BF-Control due to the low young's modulus of the BFRP bar. The first crack was extended up to a point higher than half of the slab thickness at the bottom side due to the pure bending moment in the middle zone. By increasing the applied load, more intensive cracks appeared then RC slabs failed. The crack pattern was classified as flexural failure in both. S-BF-10%-Int. and S-BF-50%-Int. cracked in the same crack distribution as mentioned in previous RC slabs (**Figs. 10 and 11**) but the cracks widened and propagated upward followed by crushing in concrete due to the post-tensioning system. S-BF-50%-Int. achieved more ultimate load than S-BF-10%-Int. due to higher stress levels in the BFRP bars. The vertical deflection was limited due to the post-tensioning system which reduced the vertical deflection, and the crack pattern was classified as crushing flexural failure.

It appeared from **Fig. 12**, that the RC slab S-St-BF-zero%-Ext. cracked with a combined crack distribution between S-St-Control and S-BF-Control. The performance of the RC slab enhanced in case of ultimate load and vertical deflection controlled due to strengthening. It's similar to S-St-Control but with a lower value of vertical deflection. The cracking behavior is controlled due to hybrid reinforcement which leads to more serviceability limits and cracks pattern classified as a flexural failure. S-St-BF-10%-Ext. and S-St-BF-30%-Ext. achieved the more significant performance. In all tested post-tensioned RC slabs, the cracks widened and propagated upward followed by crushing in concrete due to the post-tensioning system, and appeared clearly by increasing the level of stress in the post-tensioning bars. S-St-BF-30%-Ext. made the most of the post-tensioning system and that was confirmed by the final failure shape of the RC tested slab, the crack pattern classified as crushing flexural failure, see **Figs. 13 and 14**. S-St-BF and S-St-St are also cracked as RC slab S-St-BF-zero%-Ext. but S-St-BF recorded more vertical deflection and less ultimate load observed, the crack pattern was classified as a flexural failure, see **Figs. 15 and 16**.

Fig. 8: Crack pattern for RC slab, S-St-Control

Fig. 9: Crack pattern for RC slab, S-BF-Control

Fig. 10: Crack pattern for RC slab, S-BF-10%-Int.

Fig. 11: Crack pattern for RC slab, S-BF-50%-Int.

Fig. 12: Crack pattern for RC slab, S-St-BF-zero%-Ext.

Fig. 13: Crack pattern for RC slab, S-St-BF-10%-Ext.

Fig. 14: Crack pattern for RC slab, S-St-BF-30%-Ext.

Fig. 15: Crack pattern for RC slab, S-St-BF

Fig. 16: Cracks pattern for RC slab S-St-St

5. Analytical Calculations for Stress Losses and Experimental Recorded Strain

The maximum stress factor in BFRP under serviceability limit loads state still under consideration but it's more than GFRP. For GFRP, it is shall not less than 35% of environmental factor (CE), in case of creep-rupture, and cyclic-fatigue **[19]**. The environmental factor based on the location of FRP in the application (exterior or interior). Wherefore, the ratio of the maximum stress of GFRP was extrapolated to be approximately 30% **[32-33]**.

The stress losses for the post-tensioning system is the reduction of tensile stress in the bar, which in turn reduces the total prestressing force. Losses classified as two categories, the first category is the

immediate losses such as anchorage slip losses, elastic shortening losses, and friction losses. The second category is the time dependent losses such as shrinkage losses, creep losses, and relaxation losses. In the current study, threaded part of anchorage system was manufactured with tight threads to prevent the washer and nuts motion after applying post-tensioning stress. Hence, the anchorage slip losses were neglectable value. Elastic shortening losses in case of a one-step load can be taken as zero and that's what was done. Friction losses was neglected because the post-tensioning unbonded loads applied by torque keys without jack internal friction loss or wobble friction losses. Also, the bars oriented in a straight line without curvature friction losses.

Concrete shrinkage is described as a reduction in the volume of concrete that isn't caused by externally imposed forces or temperature changes and is primarily the result of moisture evaporating during drying. Hence, the shrinkage for post-tensioning RC is ordinarily taken as $200x10^{-6}$ mm/mm **[15]**. Creep is the concrete deformation with time when subjected to sustained loads. Creep is typically attributed to moisture loss, viscous flow or sliding between the gel particles, internal movement of adsorbed water, and the development of microcracks. The stress loss caused by concrete creep depends on changes in the stress levels, which occur continuously over the structure's lifetime. The creep strain value was calculated for post-tensioned RC slabs and doesn't need any corrections because the working stress at any section, f_c, doesn't exceed a third of the characteristic concrete strength, f_{cu} **[15]**.

Relaxation losses in FRP depend on many factors such as relaxation of polymer (R_p), straightening of fibers (R_s), and relaxation of fibers (R_f). According to **[17]** and **[34]**, the polymer matrix relaxes and loses its contribution to the load-carrying capacity over time within the first 24 to 96 hrs. Straightening of fibers (R_s), the fibers in a pultruded section are nearly, but not completely, parallel. Therefore, stressed fibers flow through the matrix and straighten, and this straightening appears as a relaxation loss. Straightening of the fibers is a function of the quality control of the pultrusion process. Relaxation of fibers (R_f), Fiber relaxation is dependent on the fiber type. Carbon fibers are reported to have no relaxation and may be assumed to be zero. In contrast to other types of FRP, creep behavior is slightly reflected in its relaxation behavior. However, till this time no evident equation to calculate the relaxation of fibers losses. On the other hand, the relaxation of the FRP in the Canadian Code Provisions is based on the semi-logarithm equation for different types of FRP (CFRP and AFRP).

The international codes recommended calculating shrinkage losses, and creep losses in steel post-tensioning bars by replacing material properties of steel with the used FRP material **[17 and 19]**. The following **Equations 1, 3, and 4** belong to **[15]**. Also, **Equation 1** is similar to **[18]**, and **[19]**. **Equations 2 and 5** belong to **[16]**.

5.1. Calculation of Shrinkage Losses:

$$\Delta f_{psh} = \varepsilon_{sh} E_p \qquad \textbf{Equation 1}$$

$$\Delta f_{pSH} = 8.2x10^{-6} k_{sh} E_p (1 - 0.0024v/s)(100 - RH) \qquad \textbf{Equation 2}$$

Where:

Δf_{psh} is the loss in prestress due to shrinkage

ε_{sh} is the shrinkage strain of concrete

E_p is the modulus of elasticity of the prestressing bars

k_{sh} is the shrinkage coefficient, taken as 1.0

v/s is the volume to surface ratio

RH is the humidity factor, taken as 75

5.2. Calculation of Creep Losses:

$$\varepsilon_{\text{cr}} = 36x10^{-6}\left(\frac{40}{f_{ci}}\right) \qquad \textbf{Equation 3}$$

$$\Delta f_{pcr} = \varepsilon_{cr} E_p \qquad \textbf{Equation 4}$$

$$\Delta f_{pCR} = k_{\text{cr}}\left(\frac{E_p}{E_c}\right) f_{cpa} \qquad \textbf{Equation 5}$$

Where:

ε_{cr} is the creep strain in case of compressive strength less than 35MPa

f_{ci} is the concrete strength at the beginning of prestressing (MPa)

Δf_{pcr} is the loss in prestress due to creep

E_p is the modulus of elasticity of the prestressing bars

E_c is the modulus of elasticity of the concrete

K_{cr} is the shrinkage coefficient and taken as 1.6

f_{cpa} is the concrete compressive stress at the center of gravity of the bar immediately after the prestress has been applied to the concrete

5.3. Relaxation Losses:

Relaxation of steel is totally covered by international codes. The following **Equation 6** belongs to **[15]**, and **[16]** which is used to calculate the relaxation in the prestressing steel bar.

$$\Delta f_{pr}(t) = \frac{f_{pi}(\log t)}{k_1}\left(\frac{f_{pi}}{f_{py}} - 0.55\right) \qquad \textbf{Equation 6}$$

Where:

Δf_{pr} is the loss in prestress due to the relaxation of the prestressing bar

t is the time since the beginning of tensioning in hours (max. 1000 hours)

f_{pi} is the stress in the pre-stressing bar after initial losses but before the occurrence of time-dependent losses

f_{py} is the yield stress of the pre-stressing bars

k_1 is a coefficient that depends on the type of bar, taken as 45 for low relaxation stress-relieved bar **[15],** and the same **Equation 6 [16]** written with value of 45.

The BFRP bars were tested by **[1]** under axial prestressing force and measured the elongation over time up to 30 days. The relationship in **Fig. 17** shows almost similar elongation behavior for steel bars in comparison to BFRP bars, especially if the used BFRP bars with higher volume fraction (0.71). Consequently, **Equation 6** of the relaxation losses for steel may be applied for FRP and verify with actual measured values in the BFRP bars.

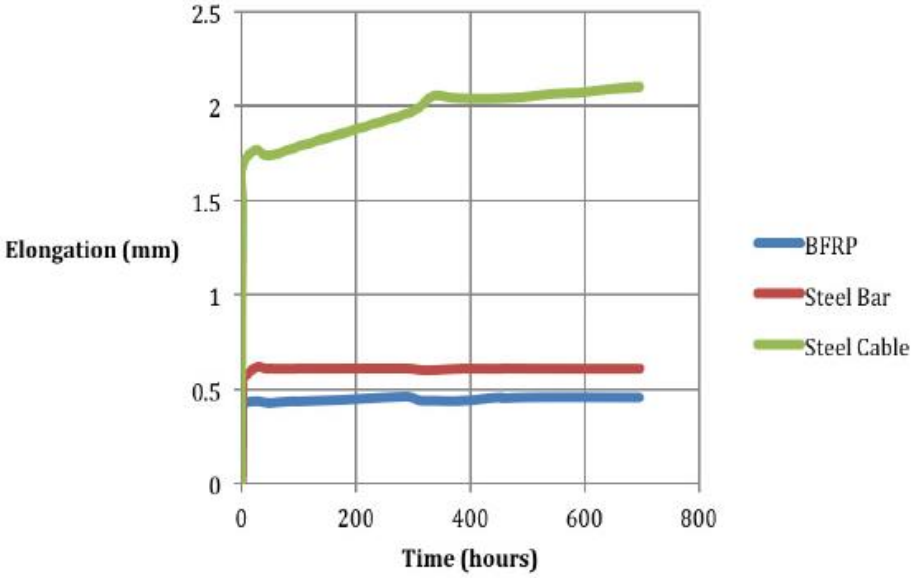

Fig. 17: Change in elongation of materials over time (30 Days) [1]

On the other hand, according to **[17]** and **[34]**, the polymer relaxation (R_p) of FRP as discussed before may be calculated based on the following **Equation 7**.

$$R_p = \frac{E_r}{E_f} v_r \qquad \textbf{Equation 7}$$

Where:

R_p is the loss in prestress due to the polymer relaxation of the prestressing bar

E_r is the young's modulus of resin matrix

E_f is the young's modulus of fiber

v_r is the volume of resin matrix

The straightening of fibers (R_s) may be taken as 1 to 2% relaxation to predict this phase of the loss calculation according to **[17]**, and **[34]**. Hence, fiber relaxation (R_f) is still under consideration.
In order to verify the calculated data, the strain in the post-tensioning bars was measured after 7 and 28 days from the concrete cast (68 hrs. and 572 hrs., after installing the post-tensioning system). **Table 10** shows that the experimentally measured strain was closer enough to the calculated strain by using code equations **[15-17]**, and that confirms the equations in calculating stress losses in BFRP bars. It's relevant that the experimentally measured strain is more than or equal to the calculated strain in both methods. Consequently, the code equation may give conservative values in an acceptable range of variation. The code Equations **[17]** gave expected out-of-range retained strain values more than the experimental and analytical values **[15-16]** due to the ignored term of fiber relaxation.

Table 10: Strain variation over time between experimental and analytical

Slab Code	Period (hrs.)	$\varepsilon_{Experimental}$ or $\varepsilon_{Analytical}$ ($x10^{-3}$) [15]	$\varepsilon_{Experimental}$ or $\varepsilon_{Analytical}$ ($x10^{-3}$) [16]	$\varepsilon_{Experimental}$ or $\varepsilon_{Analytical}$ ($x10^{-3}$) [17]
S-BF-10%-Int.	0	1.50 [2]	1.50 [2]	1.50 [2]
	68	1.26 [3]	1.26 [3]	1.26 [3]
	68	1.23 [4]	1.25 [4]	1.44 [1]
	100	1.23 [4]	1.25 [4]	1.44 [1]
	572	1.25 [3]	1.25 [3]	1.25 [3]
	572	1.22 [4]	1.24 [4]	1.44 [1]
	1000	1.21 [4]	1.23 [4]	1.44 [1]
S-BF-50%-Int.	0	7.50 [2]	7.50 [2]	7.50 [2]
	68	7.25 [3]	7.25 [3]	7.25 [3]
	68	7.24 [4]	7.19 [4]	7.21 [1]
	100	7.24 [4]	7.19 [4]	7.21 [1]
	572	7.24 [3]	7.24 [3]	7.24 [3]
	572	7.24 [4]	7.19 [4]	7.21 [1]
	1000	7.23 [4]	7.18 [4]	7.21 [1]
S-St-BF-10%-Ext.	0	1.50 [2]	1.50 [2]	1.50 [2]
	68	1.25 [3]	1.25 [3]	1.25 [3]
	68	1.23 [4]	1.25 [4]	1.44 [1]
	100	1.23 [4]	1.25 [4]	1.44 [1]
	572	1.24 [3]	1.24 [3]	1.24 [3]
	572	1.22 [4]	1.24 [4]	1.44 [1]
	1000	1.21 [4]	1.23 [4]	1.44 [1]
S-St-BF-30%-Ext.	0	4.50 [2]	4.50 [2]	4.50 [2]
	68	4.21 [3]	4.21 [3]	4.21 [3]
	68	4.21 [4]	4.20 [4]	4.33 [1]
	100	4.21 [4]	4.20 [4]	4.33 [1]
	572	4.20 [3]	4.20 [3]	4.20 [3]
	572	4.19 [4]	4.18 [4]	4.33 [1]
	1000	4.18 [4]	4.17 [4]	4.33 [1]

[1] Ignored the relaxation of fibers, and based on low quality control (2%) losses.
[2] The applied strain. [3] The measured strain. [4] The calculated strain.

It appeared from **Fig. 18** that the analytical strain **[16]** was nearest to the experimental strain compared with **[15]**, and the most stress losses happened after 68 hrs. with 16.00% (experimental). The slope of the analytical retains strain in the interval of 68 hrs. to 1000 hrs. decreased slightly. Further, the RC slab with a 10% internal stress level continued to lose its capacity analytically with time. In contrast to the RC slab with a 50% internal stress level, the slope at the same interval almost constant, and that means it's retains more strain capacity. According to the **[15]**, the analytical strain was compatible with the experimental strain, see **Fig. 19**. The RC slab lost 3.00% (experimental) of the applied strain after 68 hrs. Again, the analytical strain according to **[16]** was the nearest to the experimental strain for the RC slab with a 10% external stress level, and the analytical slope of the retained strain trended typically as RC slab with a 10% internal stress level, see **Fig. 20**. Further, the RC slab lost 16.67% (experimental) of the applied strain after 68 hrs. According to **[15]**, the analytical strain was nearest to the experimental strain for the RC slab with an external stress level of 30%. The stress losses were 6.44% (experimental) after 68 hrs, and the slope of the analytical retain strain was decreased slightly at the interval of 68 hrs to 1000 hrs, which means the RC slab with a 30% external stress level continued to lose its capacity over time

analytically, see **Fig. 21**. Ultimately, the observed and conducted results confirms that the BFRP lose almost the largest value of stress losses after almost three days, then retain the most of the strain.

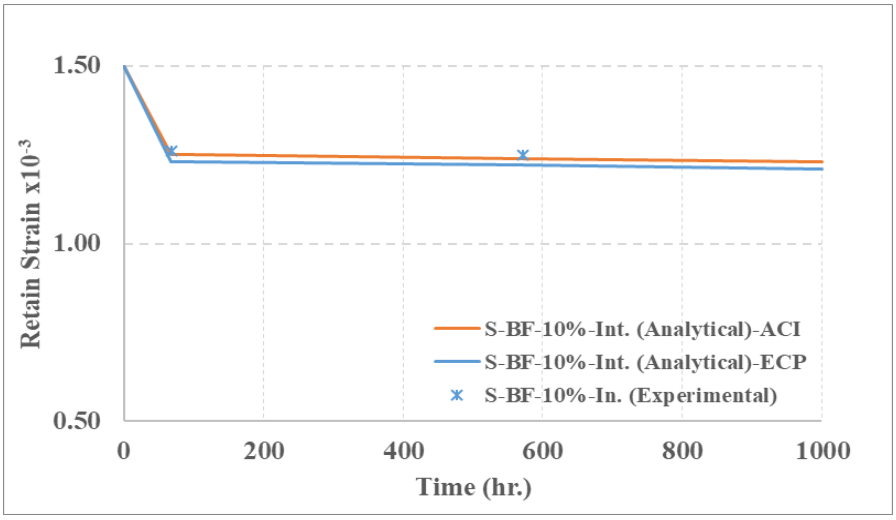

Fig. 18: Relationship between experimental and analytical results for RC slab s-bf-10%-int.

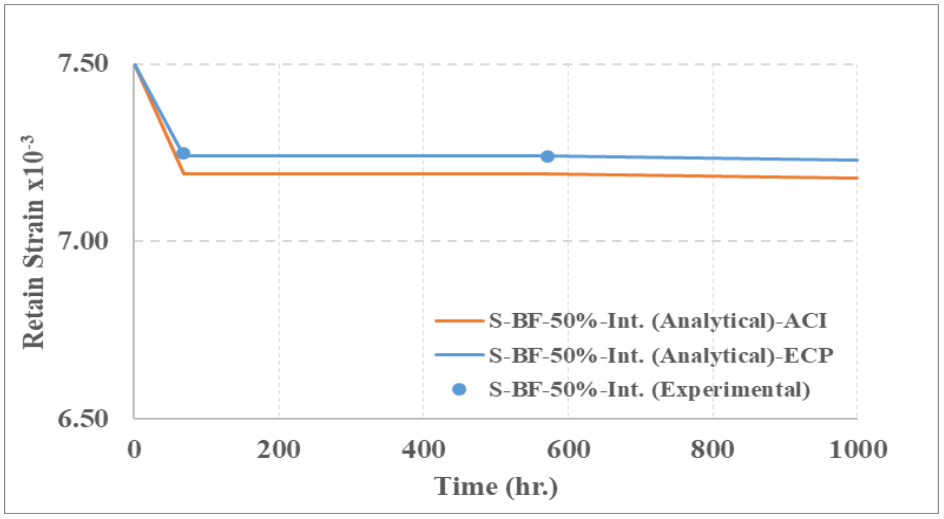

Fig. 19: Relationship between experimental and analytical results for RC slab S-BF-50%-Int.

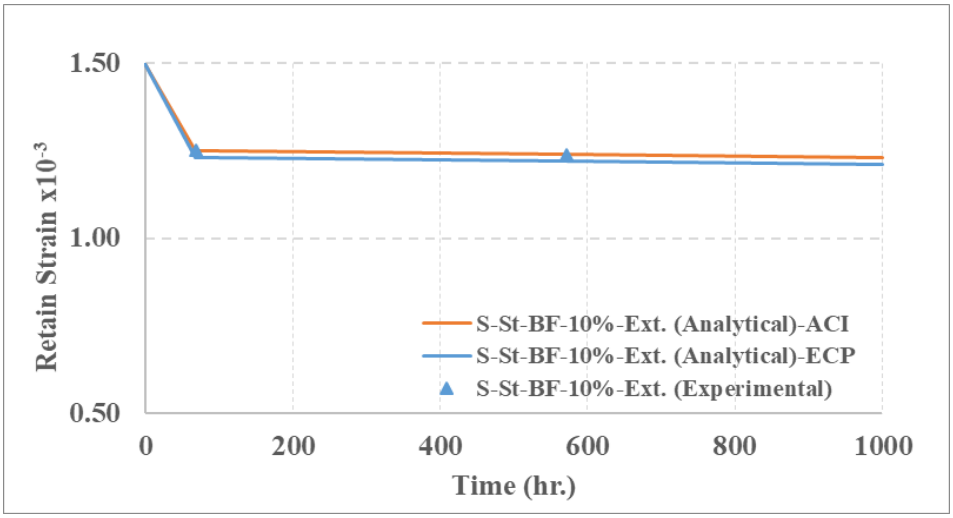

Fig. 20: Relationship between experimental and analytical results for RC slab S-BF-10%-Ext.

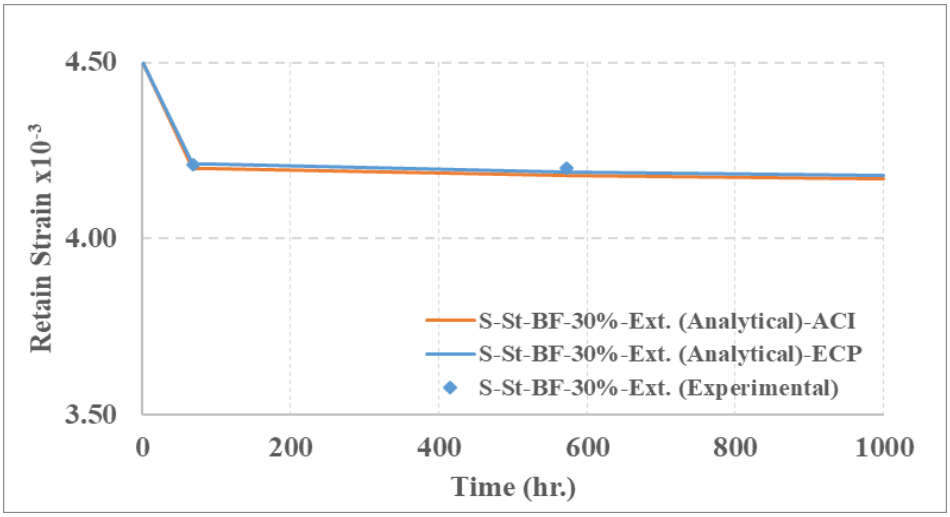

Fig. 21: Relationship between experimental and analytical results for RC slab S-BF-30%-Ext.

Table 11 shows the calculated losses for the tested RC slabs according to **[16]**, and also represents the efficiency of the post-tensioning system for BFRP bars up to 1000 hrs. It seems that by increasing the prestressing level in the BFRP bars, the losses increased with a lower rate of increase compared with the lower prestressing level (i.e., in the case of external post-tensioning with a 10% stress level, the losses were 14.11MPa after 100 hrs., and this loss occupies 16.90% of the stress level in the BFRP bars but for the level of stress 30% the losses were 16.95MPa and this loss occupies 6.77% of the stress level). Consequently, the efficiency of the post-tensioning system increased. On the other hand, the effective depth variation of the post-tensioning bars between internal and external slightly affect the stress losses. It is worth mentioning that the efficiency reduction in the post-tensioning system ranged from 4.11% to 16.90% for 100 hrs., and 4.22% to 17.89% for 1000 hrs. according to stress levels in BFRP bars, and that also complies with **[14]** and **[35]**.

Table 11: Stress losses in the post-tensioning system

Slab Code	Stress Level (MPa)	Stress Losses (MPa)					Total Losses (MPa) *100hrs.*	Total Losses (MPa) *1000hrs.*	Efficiency of Post-Tensioning System (%) *100hrs.:1000hrs.*
		Δf_{pe}	Δf_{psh}	Δf_{pcr}	$\Delta f_{pr}(t)$ *t=100hrs.*	$\Delta f_{pr}(t)$ *t=1000hrs.*			
S-BF-10%-Int.	83.5	0	11.29	0.98	1.67	2.50	13.94	14.77	83.31 : 82.31
S-BF-50%-Int.	417.5	0	11.29	4.94	0.93	1.39	17.16	17.62	95.89 : 95.78
S-St-BF-10%-Ext.	83.5	0	11.29	1.15	1.67	2.50	14.11	14.94	83.10 : 82.11
S-St-BF-30%-Ext.	250.5	0	11.29	2.88	2.78	4.17	16.95	18.34	93.23 : 92.68

Fig. 22 shows the structural performance of the prestressing system for tested post-tensioned RC slab according to **[16]**, and it appeared that the internal and external post-tensioning systems for RC slabs stressed by a 10% level of stress almost the same performance with little difference due to more effective depth for external post-tensioning RC slab. On the other hand, the post-tensioning system achieved the maximum efficiency for S-BF-50%-Int. and S-St-BF-30%-Ext. RC slabs compared with S-BF-10%-Int. and S-St-BF-10%-Ext. At the interval of 100 hrs. to 1000 hrs, the reduction rate in the efficiency of the post-tensioning system decreased. Therefore, that was confirmed by **[13]**.

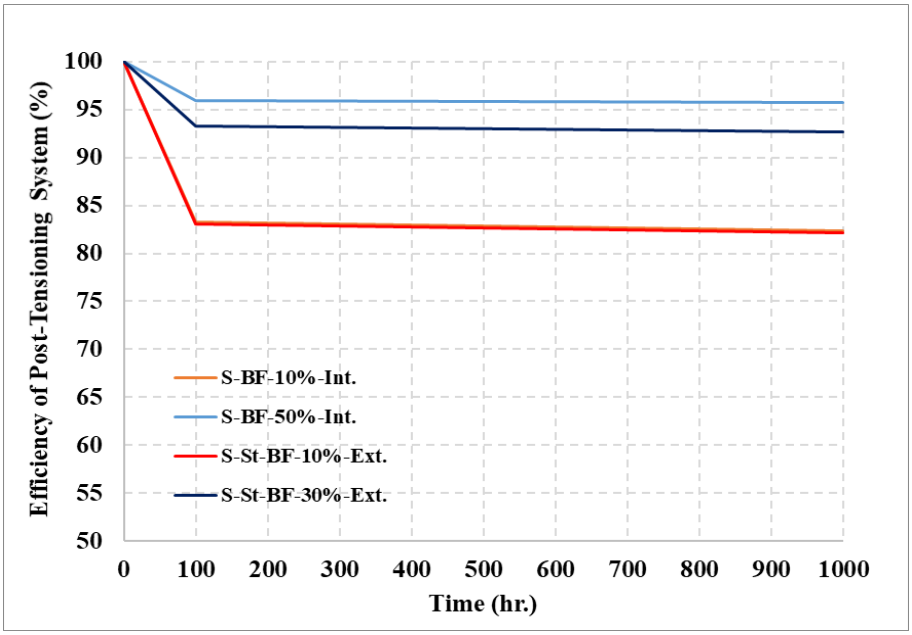

Fig. 22: Efficiency of post-tensioning system with time (hrs.)

6. Correlate the RC Slabs that are Closer in the Structural Behaviour

In this section, the tested RC slabs correlated to obtain the similarity of the RC slabs closer to each other. It was appeared from **Table 12** that the use of the BFRP bar was not recommended to add singly or post-tensioning internally with 10%, the benefits of BFRP don't appear significantly in these RC slabs, but if the level of stress increases to 50% internally, the significate benefits appear. The RC slab with steel reinforcement and strengthened externally with NSM post-tensioning BFRP bars at a stress level of 10% equal in the ultimate load to the RC slab with BFRP bars post-tensioning internally at a level of stress of 50% while achieving less vertical deflection in favor of the RC slab with steel reinforcement and strengthened externally with post-tensioned BFRP bars at a stress level of 10% by 50%. Moreover, the RC slab with a hybrid reinforcement gave almost a similar performance as the RC slab with steel reinforcement but with a higher ability to absorb energy if the proportion area of BFRP reinforcement was 40% of the area of the main reinforcement of the tested slab.

Table 12: The tested RC slabs that are closer in the structural behavior

Slab Code	Recommendation	Slab Code Correlate to	Remarks
S-St-Control	-	S-St-BF-zero%-Ext.	The same load with low vertical deflection
S-BF-50%-Int.	Highly Recommended	S-St-BF	The same load with the same vertical deflection
S-St-BF-zero%-Ext.	-	S-St-Control	The same load with the larger vertical deflection
S-St-BF-10%-Ext.	-	S-BF-50%-Int. S-St-BF	The same load with the larger vertical deflection
S-St-BF-30%-Ext.	Highly Recommended	-	-
S-St-BF	Highly Recommended	S-BF-50%-Int.	The same load with the lower vertical deflection

7. Conclusions

The efficiency of using sustainable BFRP bars as an external or internal post-tensioning system in RC Slabs during the short-term period was investigated on different sides and the flexural behavior of the RC slabs with BFRP bars (internally or externally), hybrid reinforcements (steel and BFRP bars) and, steel reinforcement (A_s) were experimentally investigated and stress losses analytically calculated according to different international codes. Based on the results obtained, the following conclusions can be drawn:

- The steel grip 300mm in length, 200mm (plain-hollow inside), and the left 100mm thread for nut fixation is an innovative fixation setup to overcome unthreadable BFRP bars of prestressing systems.
- The ultimate load for the control RC slab with steel reinforcement increased by 119.19% and 47.11% compared to the RC slab with internal BFRP reinforcement bars or post-tensioning internally with a stress level of 10%. Therefore, the ultimate load increased for the internally post-tensioned RC slab by 50% more than the RC slab with steel reinforcement by 8.35% in addition to ductility value compared with the rest of the tested RC slabs.
- By increasing the stress level of BFRP post-tensioning bars, the ultimate load of the RC slab increased. The ultimate load for the RC slab with internally post-tensioning BFRP bars with a stress level of 50% is almost 59.40% more than that of the RC slab with a 10% stress level of post-tensioning internally BFRP bars.
- The benefits of using BFRP bars as NSM in external post-tensioned RC slabs significantly appeared. In this regard, by increasing the stress levels in BFRP bars from 10% to 30%, the ultimate load increased by 28.24%, the vertical deflection decreased by 22.90%, and the ultimate load increased rather than the RC slab with steel reinforcement by 6.93% and 37.13%, respectively. Moreover, by increasing the stress level of the external post-tensioning BFRP bars from 10% to 30%, the ultimate load of the strengthened RC slab increased by 10.29% and 41.44%, respectively compared to the RC slab strengthened externally with a zero% level of stress of post-tensioning BFRP bars.
- Adding BFRP bars as 40% of the total reinforcement area almost gave the ultimate load and (P_{cr}/P_u) ratio as the same as the RC slab with the same reinforcement area (μ=0.65%) without BFRP reinforcement but with higher vertical deflection and more energy can absorb. Also, the bonded BFRP bars achieved a higher ultimate load for the RC slab than unbonded BFRP bars by 11.76% at the same reinforcement area (μ=0.65%).
- The RC slab with steel reinforcement or internally reinforced with bonded BFRP bars have the same crack distribution, and the crack pattern was flexural failure in both and the same for the RC slab with hybrid reinforcements, while the crack pattern was crushing flexural failure for the post-tensioned RC slabs with BFRP bars.
- The RC slab with steel reinforcement and strengthened externally with NSM post-tensioning BFRP bars at a stress level of 10% can be correlated in the ultimate load to the RC slab with internally post-tensioning BFRP bars at a stress level of 50%. Hence, it is recommended to post-tensioning the BFRP bars with at least a 30% stress level.
- The hybrid RC slab absorbed more energy than the steel RC slab by 85.06% in addition to achieving more ductility by 191.26% and the same trend in the ultimate load, stiffness in all stages, which fulfills the benefits of hybrid reinforcement by adding BFRP bars with 40% of the total reinforcement area which achieved the promising enhancement.
- The effective depth of the post-tensioning system between internal and external slightly affects the stress losses, and by increasing the prestressing level in BFRP bars, the losses increased at a lower rate compared with lower stress levels. Wherefore, the efficiency of the

external post-tensioning system was 95.78% for the RC slab with a 50% stress level after 1000 hrs.

References

[1] P. Maximus, D. Ted, and S. Juan, "Long-Term Behaviour of Prestressed Basalt Fibre Reinforced Polymer Bars", The 2nd International Conference on Rehabilitation and Maintenance in Civil Engineering, Procedia Engineering 54 (2013), 261 – 269.

[2] B. Pouya, P. Anil, "Creep Rupture Performance of Basalt Fiber-Reinforced Polymer Bars", J. Aerospace Engineering 28(2013):04014074.

[3] P. Ana, D. Ted, P. Diana, and L. Mukesh, (2022), "Short- and Long-Term Prestress Losses in Basalt FRP Prestressed Concrete Beams under Sustained Loading", J. of Composites for Construction, 26 (2022), https://doi.org/10.1061/(ASCE)CC.1943-5614.0001259.

[4] I. Marianne, R. T. Eythor, A. Kamal, "A Mechanical and Environmental Assessment and Comparison of Basalt Fibre Reinforced Polymer (BFRP) Rebar and Steel Rebar in Concrete Beams", Energy Procedia, 111(2017), 31-40

[5] X. Wang, J. Shi , Z. Wu, Z. Zhu, "Creep strain control by pretension for basalt fiber-reinforced polymer tendon in civil applications" 89(2016), 1270–1277.

[6] J. Shi, X. Wang, H. Huang, Z. Wu, "Relaxation behavior of prestressing basalt fiber-reinforced polymer tendons considering anchorage slippage", Journal of Composite Materials, 51(2016), 1275–1284, https://doi.org/10.1177/0021998316673893.

[7] A. Gunnarsson (2013), "Bearing capacity, relaxation and finite element simulation for prestressed concrete beams reinforced with BFRP tendons". Master Thesis, Reykjavik University, Iceland.

[8] G. Tao, P. Zhuge, D. Lin, T. Zeng "Study on short-term prestress loss of bridge reinforced with large diameter carbon fiber bars", International Conference on Mechanics and Civil, Hydraulic Engineering, IOP Conf. Series: Earth and Environmental Science 820 (2021) 012001, IOP Publishing.

[9] A. Kovalovs, P. Akishin, A. Chate, "Detection Prestress Loss in Prestressed Concrete Slab using Modal Analysis", IOP Conf. Ser.: Mater. Sci. Eng (2019). 471 102015.

[10] G. Ghanem, S. Abd El-Bakey, T. Ali, and S. Yehia, "Behavior of RC Beams Retrofitted/Strengthened with External Post-Tension System", International Journal of Civil, Mechanical and Energy Science, 2(2016), 36-43.

[11] Danying Gao, Dong Fang, Peibo You, Gang Chen, Jiyu Tang, (2020), "Flexural behavior of reinforced concrete one-way slabs strengthened via external post-tensioned FRP tendons", Engineering Structures, 216 (2020) 110718, https://doi.org/10.1016/j.engstruct.2020.110718.

[12] A.V. Oskouei, S.M. Taleie, "Experimental Investigation on Relaxation of Fiber reinforced Polymer Composites", Journal of Reinforced Plastics and Composites, 29 (2010), 2705-2718.

[13] M. Przygocka, R. Kotynia, "Pre-Stress Losses in FRP Pre-Stresses Reinforced Concrete – Subject Overview", Archives of Civil Engineering, 64(2018), 257-268, DOI:10.2478/ace-2018-0073.

[14] X. Wang, J. Shi, J. Liu, L. Yang, Z. Wu, "Creep behavior of basalt fiber reinforced polymer tendons for prestressing application", Mater. Des. 59 (2014) 558–564.

[15] ECP:203-2020, "Egyptian Code of Practice for Reinforced Concrete Construction", Housing and Building National Research Center, (HBRC).

[16] ACI:423.10R-16, "Guide to Estimating Prestress Losses", American Concrete Institute Committee Report.

[17] ACI:440.4R-04 (R2011), "Prestressing Concrete Structures with FRP Tendons" American Concrete Institute Committee Report.

[18] CSA-A23.3-19, "Design of concrete structures" Canadian Standards Association.

[19] CSA-S806-12 (R2021), "Design and construction of building structures with fibre-reinforced polymers", Canadian Standards Association.

[20] ES:1109/2021, "Egyptian Standards for Natural Aggregate", Egyptian Organization for Standards & Quality.

[21] ES:4756-1/2022, "Egyptian Standards for Cement", Egyptian Organization for Standards & Quality.

[22] BS:8500-2019, "British Standard for Concrete Mix Design" Concrete – Complementary British Standard to BS EN 206.
[23] H. Wang, "Discussion of "Bond Behavior of Fiber Reinforced Polymer Bars under Direct Pullout Conditions" by Zenon Achillides and Kypros Pilakoutas. 8(2004), 173–181.
[24] Sikadur-31 CF, data sheet, www.sika.com.
[25] ACI:440.3R-12, "Guide Test Methods for Fiber-Reinforced Polymer (FRP) Composites for Reinforcing or Strengthening Concrete and Masonry Structures" American Concrete Institute Committee Report.
[26] ASTM: D7205/D7205M-06, "Standard Test Method for Tensile Properties of Fiber Reinforced Polymer Matrix Composite Bars", American Society for Testing and Materials.
[27] CSA-S807:19, "Specification for fibre-reinforced polymers", Canadian Standards Association.
[28] ES:262/2021, "Egyptian Standards for Steel Reinforcement", Egyptian Organization for Standards & Quality.
[29] ASTM A615, A615M-04A, Standard Specification for Deformed and Plain Billet-Steel Bars for Concrete Reinforcement, American Society for Testing and Materials.
[30] BS:12390-3-2002 "Testing Hardened Concrete. Compressive Strength of Test Specimens" British Standards Institution.
[31] S. Abd El-Baky, S. Yehia, A. M. A. Ibrahim, and A. Haded "Effect of BFRP Post Tensioning System on Hybrid Reinforced Concrete Slab", International Journal of Scientific & Engineering Research - IJSER, 12(2021), 432-437.
[32] ACI:440.2R-17, "Guide for the Design and Construction of Externally Bonded FRP Systems for Strengthening Concrete Structures" ACI Committee 440, American Concrete Institute.
[33] ECP:208-2019, "Egyptian Code of Practice for design principles and requirements for the implementation of fiber reinforced polymers in the field of construction", Housing and building national research center, (HBRC).
[34] C.W. Dolan, H.R. Hamilton, C.E. Bakis, and A. Nanni, (2000), "Design Recommendations for Concrete Structures Prestressed with FRP Tendons, Final Report," Department of Civil and Architectural Engineering Report DTFH61-96-C- 00019, University of Wyoming, Laramie, Wyo., May, 113 pp.
[35] A. Pavlović, T. Donchev, D. Petkova, M. Limbachiya, "Short and long-term prestress losses in basalt FRP prestressed concrete beams under sustained loading", Journal of Composites for Construction, 26 (2022), https://doi.org/10.1061/ (ASCE)CC.1943-5614.0001259.